Journal of Artificial Intelligence and Data Science (JAIDA)
e-ISSN: 2791-8335
https://dergipark.org.tr/pub/jaida

Vol. 4, No. 2, pp. 68-78, 2024
Research Article
Received: 06/11/2024 Accepted: 12/12/2024

Optimization of Thermal Management for Cooling System of Power Electronics Modules Consisting Insulated-Gate Bipolar Transistor Using Neuro-Regression Analysis and Non-Traditional Algorithms

Melih SAVRAN[1,*], Ece Nur YÜNCÜ[2] , Levent AYDIN[3]

Abstract

Thermal management and extreme temperatures critically influence the performance of power electronics systems, especially those utilizing Insulated-Gate Bipolar Transistors (IGBTs) and diode components. Various parameters govern the cooling efficiency of these systems. In this study, the IGBT temperature was selected as the objective function. To achieve temperature minimization, optimum values of design variables: coolant flow rate (L/min), distance from the vortex generator (mm), height (µmm), and width of the first pin-fin (µmm), and distance of the vortex generator from the surface (µmm) were determined. The mathematical modeling process employed Neuro-Regression analysis. The prediction performance of proposed 14 different regression models was evaluated using R^2Training, R^2Testing, R^2Validation indexes and boundedness check criteria. Differential Evolution, Nelder Mead, Simulated Annealing, and Random Search algorithms were applied to minimize IGBT temperature. The First Order Logarithmic Nonlinear (FOLN) model emerged as the most successful, achieving a minimum temperature lower than the experimental dataset given in literature. The results indicate a 12 % reduction in the minimum IGBT temperature.

Keywords: Optimization, neuro-regression analysis, thermal management, IGBT, cooling system

1. Introduction

Effective thermal management systems are essential for the practical use of lithium-ion battery packs. Air cooling alone is insufficient to maintain battery pack temperatures within a safe operating range under high-stress conditions without substantial fan power consumption [1, 2]. Insulated gate bipolar transistor (IGBT) modules have recently become prevalent in various industries, notably in high-power converters for wind turbines, trains, and HVDC systems [3]. Thermal management, encompassing battery temperature regulation and air conditioning cabinet, poses a significant challenge for electric vehicles (EVs), where traditional engines and oil tanks are replaced by electric motors and battery assemblies [4]. Optimizing thermal management is critical for the performance of IGBT-based power modules in hybrid electric vehicles [5]. Jun He et al. have studied the thermal design and assessment of IGBT power modules under both transient and steady-state conditions, suggesting that optimizing wire bond configurations and bonding pad positions can significantly reduce temperature gradients and peak temperatures on the IGBT surface [6]. Thermal resistance (Rth), defined as the ratio of the temperature difference between the heat output and input ends to the power, is a crucial parameter for IGBT modules and an important measure of their heat dissipation efficiency [7].

Efficient thermal management not only enhances performance but also enables the miniaturization of power electronics equipment [8]. In the application of IGBTs, particularly in high-voltage heater systems, the challenge lies in managing the additional heat generated by the heating elements applied via plasma deposition technology. This makes the thermal management requirements even more stringent. In the application of an IGBT, it is crucial to analyze the heat generation and transfer behavior to minimize chip temperature. Within a high voltage heater system, the IGBT is secured to the heat exchanger using bolts, while the heating element is directly applied to the heat exchanger using plasma deposition technology. As a result, during IGBT operation, in addition to the heat

*Corresponding author

Melih SAVRAN*; İzmir Kâtip Çelebi University, Department of Mechanical Engineering, İzmir, Türkiye; e-mail: mlhsvrn@gmail.com

0000-0001-8343-1073

Ece Nur YÜNCÜ; Izmir Kâtip Çelebi University, Department of Electrical and Electronics Engineering, İzmir, Türkiye; e-mail: ecenuryuncu79@gmail.com

0009-0002-3195-124X

Levent AYDIN; İzmir Kâtip Çelebi University, Department of Mechanical Engineering, İzmir, Türkiye; e-mail: leventaydinn@gmail.com

0000-0003-0483-0071

produced by the chip itself, heat is also transferred from the heating elements, leading to more stringent thermal management requirements for the IGBT in the high voltage heater system. Current cooling methods for IGBTs are inadequate for maintaining a safe temperature range under the high-power heating conditions of the high voltage heater system, posing a significant risk to system reliability. So far, many studies on IGBT cooling have concentrated on designing cooling structures to solve the problem of effective heat dissipation for IGBTs [9].
Rao et al. optimized a plate-fin heat exchanger by minimizing the total number of entropy generation units for a specific heat duty requirement within given space constraints, reducing the total volume, and lowering the total annual cost [10]. Lee et al. utilized a multi-objective genetic algorithm combined with surrogate modeling techniques to maximize heat transfer and minimize pressure drop in a heat exchanger [11]. Mishra et al. used GA for optimal design of plate-fin heat exchangers [12, 13]. Some authors used particle swarm optimization for rolling fin-tube heat exchanger optimization [14].

The main goal of this study is to optimize the cooling of a power electronic system that consists of an IGBT and a diode, along with the associated connections and joints, by leveraging the data from Pourfattah Farzad et al. [15]. This study introduces a novel approach to address the shortcomings in the design, modeling, and optimization of the thermal management for cooling systems of power electronics modules. The proposed method employs multiple nonlinear neuro-regression analyses, integrating artificial neural networks (ANN), regression analysis, and stochastic optimization techniques to achieve suitable designs that meet desired specifications. This approach allows for diverse alternative mathematical models, transcending traditional limitations to specific polynomial forms or activation functions such as sigmoid, unit step, and hyperbolic tangent.
Furthermore, model assessment incorporates both the R^2 value and a boundedness check criterion, which provides a more holistic evaluation of model reliability. The boundedness check is vital for developing dependable mathematical models, as all engineering parameters must be finite. Realistic modeling in engineering systems necessitates that models are bounded within specified parameter intervals; thus, verifying this boundedness prior to optimization is essential. In contrast to modeling techniques reliant on artificial neural networks, this method circumvents the need for fine-tuning parameters such as the number of neurons and hidden layers, which are often adjusted to enhance ANN-based models. This modeling approach significantly enhances the thermal management for cooling systems of power electronics module in the existing literature. Algorithms; Differential Evolution, Nelder Mead, Simulated Annealing, and Random Search are employed to identify the optimal design parameters and IGBT temperature for efficient thermal management.

2. Materials and Methods

2.1 Mathematical modelling

In the modeling stage, a combined method of regression analysis and artificial neural networks are utilized to enhance the accuracy of predictions. The dataset is divided into three parts: 80% for training, 15% for testing, and 5% for validation. During training, various regression models outlined in Table 1 were employed to minimize the disparity between experimental and predicted values. In the testing and validation phase, the objective was to generate prediction outcomes while mitigating inconsistencies among regression models. Evaluating the boundedness of the models was crucial for assessing their realism. Following the selection of suitable models based on R^2 index for training, testing, and validation, the maximum and minimum values for each design parameter were computed. In q. (1), R^2 is coefficient of determination that indicates how well the data fit a regression model. R^2 value range from 0 to 1. As R^2 value is closer to 1 it indicates that there is a good fit with that model. SSE stands for 'Sum of Squared Errors' and measures the total deviation of the observed values from the predicted values produced by the regression model. SST stands for 'sum of squares total' and measures the total deviation of the observed values from their mean.

$$R^2 = 1 - \frac{SSE}{SST} \tag{1}$$

Table 1. Multiple regression model types including
linear, quadratic, trigonometric, logarithmic, and their rational forms [16]

Model Name	Nomenclature	Formula
MultipleLinear	L	(a0 + a1 x1 + a2 x2 + a3 x3 + a4 x4 + a5 x5)
Multiple Linear Rational	LR	(a0 + a1 x1 + a2 x2 + a3 x3 + a4 x4 + a5 x5) / (b0 + b1 x1 + b2 x2 + b3 x3 + b4 x4 + b5 x5)
Second-Order Multiple Nonlinear	SON	(a0 + a1 x1 + a2 x2 + a3 x3 + a4 x4 + a5 x5 + a6 x1 x1 + a7 x2 x2 + a8 x3 x3 + a9 x4 x4 + a10 x5 x5 + a11 x1 x2 + a12 x1 x3 + a13 x1 x4 + a14 x1 x5 + a15 x2 x3 + a16 x2 x4 + a17 x2 x5 + a18 x3 x4 + a19 x3 x5 + a20 x4 x5)
Second-Order Multiple Nonlinear Rational	SONR	(a0 + a1 x1 + a2 x2 + a3 x3 + a4 x4 + a5 x5 + a6 x1 x1 + a7 x2 x2 + a8 x3 x3 + a9 x4 x4 + a10 x5 x5 + a11 x1 x2 + a12 x1 x3 + a13 x1 x4 + a14 x1 x5 + a15 x2 x3 + a16 x2 x4 + a17 x2 x5 + a18 x3 x4 + a19 x3 x5 + a20 x4 x5) / (b0 + b1 x1 + b2 x2 + b3 x3 + b4 x4 + b5 x5 + b6 x1 x1 + b7 x2 x2 + b8 x3 x3 + b9 x4 x4 + b10 x5 x5 + b11 x1 x2 + b12 x1 x3 + b13 x1 x4 + b14 x1 x5 + b15 x2 x3 + b16 x2 x4 + b17 x2 x5 + b18 x3 x4 + b19 x3 x5 + b20 x4 x5)
First-Order Trigonometric Multiple Nonlinear	FOTN	(a0 + a1 Sin[x1] + a2 Sin[x2] + a3 Sin[x3] + a4 Sin[x4] + a5 Sin[x5] + a6 Cos[x1] + a7 Cos[x2] + a8 Cos[x3] + a9 Cos [x4] + a10 Cos[x5])
First-Order Trigonometric Multiple Nonlinear Rational	FOTNR	(a0 + a1 Sin[x1] + a2 Sin[x2] + a3 Sin[x3] + a4 Sin[x4] + a5 Sin[x5] + a6 Cos[x1] + a7 Cos[x2] + a8 Cos[x3] + a9 Cos [x4] + a10 Cos[x5]) / (b0 + b1 Sin[x1] + b2 Sin[x2] + b3 Sin[x3] + b4 Sin[x4] + b5 Sin[x5] + b6 Cos[x1] + b7 Cos[x2] + b8 Cos[x3] + b9 Cos [x4] + b10 Cos[x5])
Second-OrderTrigonometric Multiple Nonlinear	SOTN	(a0 + a1 Sin[x1] + a2 Sin[x2] + a3 Sin[x3] + a4 Sin[x4] + a5 Sin[x5] + a6 Cos[x1] + a7 Cos[x2] + a8 Cos[x3] + a9 Cos [x4] + a10 Cos[x5] + a11 Sin[x1] Sin[x1] + a12 Sin[x2] Sin[x2] + a13 Sin[x3] Sin[x3] + a12 Sin[x4] Sin[x4] + a15 Sin[x5] Sin[x5] + a16 Cos[x1] Cos[x1] + a17 Cos[x2] Cos[x2] + a18 Cos[x3] Cos[x3] + a19 Cos[x4] Cos[x4] + a20 Cos[x5] Cos[x5])
Second-OrderTrigonometric Multiple Nonlinear Rational	SOTNR	(a0 + a1 Sin[x1] + a2 Sin[x2] + a3 Sin[x3] + a4 Sin[x4] +a5 Sin[x5] + a6 Cos[x1] + a7 Cos[x2] + a8 Cos[x3] + a9 Cos [x4] + a10 Cos[x5] + a11 Sin[x1] Sin[x1] + a12 Sin[x2] Sin[x2] + a13 Sin[x3] Sin[x3] + a12 Sin[x4] Sin[x4] + a15 Sin[x5] Sin[x5] + a16 Cos[x1] Cos[x1] + a17 Cos[x2] Cos[x2] + a18 Cos[x3] Cos[x3] + a19 Cos[x4] Cos[x4] + a20 Cos[x5] Cos[x5]) / (b0 + b1 Sin[x1] + b2 Sin[x2] + b3 Sin[x3] + b4 Sin[x4] + b5 Sin[x5] + b6 Cos[x1] + b7 Cos[x2] + b8 Cos[x3] + b9 Cos [x4] + b10 Cos[x5] + b11 Sin[x1] Sin[x1] + b12 Sin[x2] Sin[x2] + b13 Sin[x3] Sin[x3] + b12 Sin[x4] Sin[x4] + b15 Sin[x5] Sin[x5] + b16 Cos[x1] Cos[x1] + b17 Cos[x2] Cos[x2] + b18 Cos[x3] Cos[x3] + b19 Cos[x4] Cos[x4] + b20 Cos[x5] Cos[x5])
First-Order Logarithmic Multiple Nonlinear	FOLN	(a0 + a1 Log[x1] + a2 Log[x2] + a3 Log[x3] + a4 Log[x4] + a5 Log[x5])
First-Order Logarithmic Multiple Nonlinear Rational	FOLNR	(a0 + a1 Log[x1] + a2 Log[x2] + a3 Log[x3] + a4 Log[x4] + a5 Log[x5]) / (b0 + b1 Log[x1] + b2 Log[x2] + b3 Log[x3] + b4 Log[x4] + b5 Log[x5])
Second-Order Logarithmic Multiple Nonlinear	SOLN	(a0 + a1 Log[x1] + a2 Log[x2] + a3 Log[x3] + a4 Log[x4] + a5 Log[x5] +a6 Log[x1] Log[x1] + a7 Log[x2] Log[x2] + a8 Log[x3] Log[x3] + a9 Log[x4] Log[x4] + a10 Log[x5] Log[x5] + a11 Log[x1] Log[x2] + a12 Log[x1] Log[x3] + a13 Log[x1] Log[x4] + a14 Log[x1] Log[x5] + a15 Log[x2] Log[x3] + a16 Log[x2] Log[x4] + a17 Log[x2] Log[x5] + a18 Log[x3] Log[x4] + a19 Log[x3] Log[x5] + a20 Log[x4] Log[x5])
Second-Order Logarithmic Multiple Nonlinear	SOLNR	(a0 + a1 Log[x1] + a2 Log[x2] + a3 Log[x3] + a4 Log[x4] + a5 Log[x5] +a6 Log[x1] Log[x1] + a7 Log[x2] Log[x2] + a8 Log[x3] Log[x3] + a9 Log[x4] Log[x4] + a10 Log[x5] Log[x5] + a11 Log[x1] Log[x2] + a12 Log[x1] Log[x3] + a13 Log[x1] Log[x4] + a14 Log[x1] Log[x5] + a15 Log[x2] Log[x3] + a16 Log[x2] Log[x4] + a17 Log[x2] Log[x5] + a18 Log[x3] Log[x4] + a19 Log[x3] Log[x5] + a20 Log[x4] Log[x5]) / (b0 + b1 Log[x1] + b2 Log[x2] + b3 Log[x3] + b4 Log[x4] + b5 Log[x5] + b6 Log[x1] Log[x1] + b7 Log[x2] Log[x2] +b8 Log[x3] Log[x3] + b9 Log[x4] Log[x4] + b10 Log[x5] Log[x5] + b11 Log[x1] Log[x2] + b12 Log[x1] Log[x3] + b13 Log[x1] Log[x4] + b14 Log[x1] Log[x5] + b15 Log[x2] Log[x3] + b16 Log[x2] Log[x4] + b17 Log[x2] Log[x5] + b18 Log[x3] Log[x4] + b19 Log[x3] Log[x5] + b20 Log[x4] Log[x5])

Two new hybrid regression models are also proposed in this study. These regression model formulas are given in Table 2.

Table 2. Hybrid regression model types

Model Name	Nomenclature	Formula
Hybrid	H(FOLN+SON)	(a0 + a1 Log[x1] + a2 Log[x2] + a3 Log[x3] + a4 Log[x4] + a5 Log[x5] + a6 + a7 x1 + a8 x2 + a9 x3 + a10 x4 + a11 x5 + a12 x1 x1 + a13 x2 x2 + a14 x3 x3 + a15 x4 x4 + a16 x5 x5 + a17 x1 x2 + a18 x1 x3 + a19 x1 x4 + a20 x1 x5 + a21 x2 x3 + a22 x2 x4 + a23 x2 x5 + a24 x3 x4 + a25 x3 x5 + a26 x4 x5)
Hybrid	H(FOLN*L)	(a0 + a1 Log[x1] + a2 Log[x2] + a3 Log[x3] + a4 Log[x4] + a5 Log[x5]) * (a6 + a7 x1 + a8 x2 + a9 x3 + a10 x4 + a11 x5)

2.2 Optimization

Optimization involves refining a system or process to achieve the best possible outcome. This process entails adjusting input variables to minimize or maximize the output of a function, often referred to as the cost function, objective function, or fitness function. The goal is to optimize these inputs to achieve the best possible performance of the system [17].

2.2.1. Differential evolution

Differential Evolution (DE) is a population-based optimization algorithm particularly effective for solving complex, high-dimensional optimization problems. DE begins by initializing a population of candidate solutions, iteratively refining them across generations by exploiting differences (differentials) between solutions within the population. In each generation, new candidate solutions are generated through a mutation process, which typically involves selecting three random individuals to create differential vectors. These vectors are then combined with an existing solution to propose a new candidate. A crossover operation further enhances solution diversity, while a selection process ensures that only improved solutions are retained. One of DE's key strengths is its ability to reach globally optimal solutions without requiring gradient information, making it highly suitable for applications in engineering and scientific research. Its relatively low sensitivity to parameter settings also contributes to its widespread use in various optimization tasks [18].

2.2.2. Nelder-mead

The Nelder-Mead algorithm is a widely used direct search optimization technique that operates without the need for gradient information, making it suitable for optimizing non-differentiable or complex objective functions. The algorithm maintains a simplex—a geometric shape formed by n+1n+1n+1 vertices in an nnn-dimensional space—and iteratively refines it using four main operations: reflection, expansion, contraction, and shrinkage. Through these operations, the simplex adjusts its shape, size, and orientation dynamically, allowing it to navigate the objective function landscape effectively and converge towards a local optimum. By adapting to the contours of the objective function, the Nelder-Mead algorithm demonstrates flexibility and robustness, making it particularly valuable for challenging optimization tasks where traditional gradient-based methods may be infeasible or ineffective [19].

2.2.3. Random search

The Random Search algorithm is a stochastic optimization technique that contrasts with deterministic methods, such as Branch and Bound or Interval Analysis, by relying on random sampling rather than systematic exploration of the search space. Unlike gradient-based or small-step methods that risk converging to local optima, Random Search samples candidate solutions across the entire search domain, thereby increasing its likelihood of identifying a global optimum, especially in multimodal objective functions. This characteristic makes Random Search particularly advantageous for problems where the objective function contains multiple peaks or valleys. The algorithm's simplicity and adaptability allow it to explore complex search landscapes without gradient information, though its efficiency can be enhanced by combining it with local refinement strategies to ensure both global exploration and local exploitation of high-potential regions [20].

2.2.4. Simulated annealing

Simulated Annealing (SA) is a widely adopted optimization technique within random search methods, inspired by the physical annealing process. In this process, a metal is heated to a high temperature and then gradually cooled, allowing its atomic structure to settle into a state of lower energy, resulting in a tougher and more stable material. In the context of optimization, the SA algorithm mimics this annealing process to enable solutions to escape local minima and explore the search space more broadly in pursuit of a global optimum. Initially, the algorithm accepts a wide range of solutions, including those that may increase the objective function, which helps it to traverse diverse regions of the search landscape. As the "temperature" parameter decreases, the acceptance of higher-energy solutions becomes less likely, guiding the algorithm towards a stable and optimal solution. This dynamic makes SA particularly effective for solving complex, multimodal optimization problems, as it balances global exploration and local refinement [21].

2.3. Problem definition

The main aim of this study is to identify the optimal design parameters to minimize the temperature of the IGBT. The study involves several steps:

i) Data Selection and determination of design variables and output parameters: Data was taken from the reference study conducted by Pourfattah Farzad et al. [15]. The design variables included the coolant flow rate, the height and width of the first pin-fin attached to the heatsink, the distance from the vortex generator, the distance from the coolant path surface to the vortex generator. The output parameter is selected as IGBT temperature.

ii) Model Selection: Fourteen regression models were utilized, and their validity was assessed by checking the R^2 values and boundedness criteria. Models are considered successful when they achieve R^2 values greater than 0.85 and have realistic maximum and minimum outputs for engineering applications.

iii) Optimization: The model, which successfully met the model assessment and boundedness control criteria, was optimized using four optimization methods (DE, NM, RS, SA) to obtain optimal results, which were then compared with one another.

The flow chart in Figure 1 provides a detailed description of the steps taken in the mathematical modeling and optimization processes.

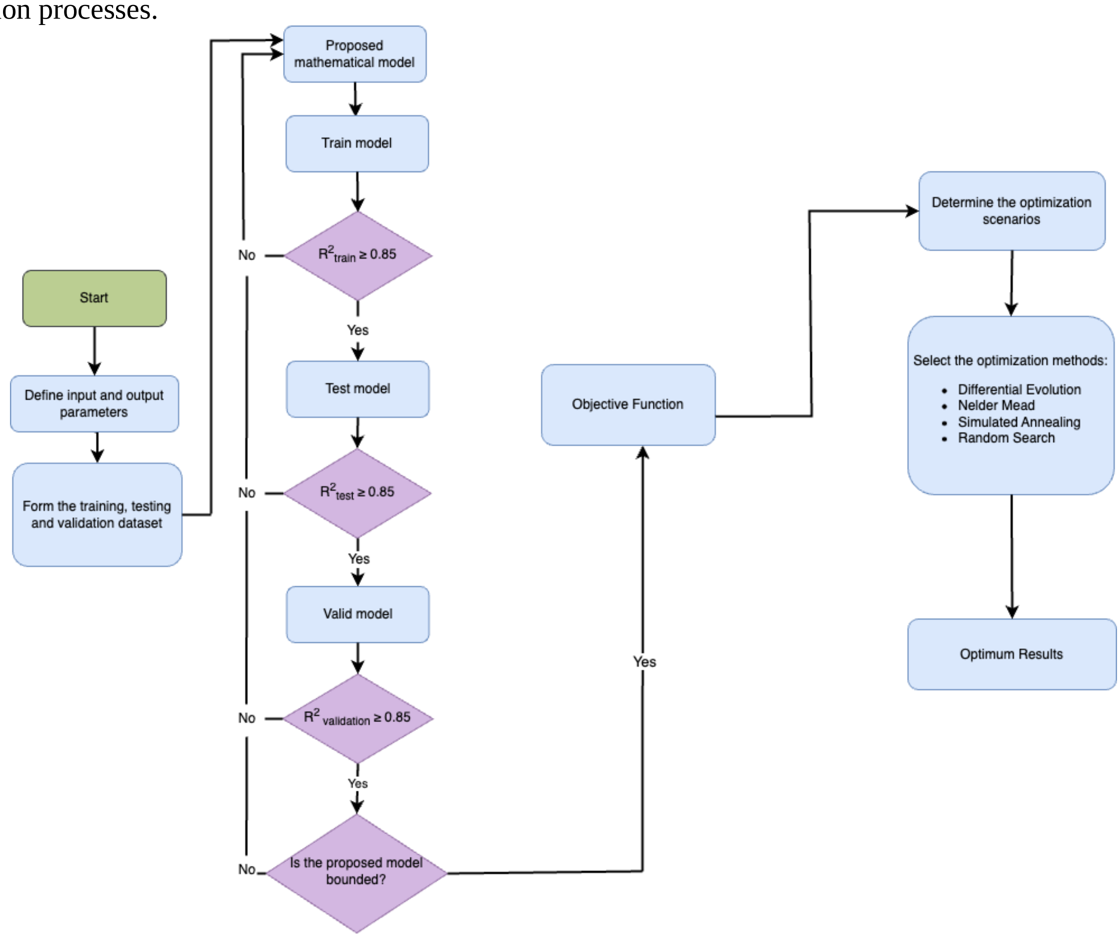

Figure 1. The flowchart regarding mathematical modeling and optimization process

2.3.1 Optimization scenarios

Three scenarios with varying constraints on the design parameters were established to determine the optimal solution.

Scenario 1

In the first scenario, the search space was continuous. The intervals for the design variables are as follows:1.203 ≤ x1 (L/min) ≤ 4.497, 505.56 ≤ x2 (μmm) ≤ 783.33, 2.215 ≤ x3 (mm) ≤ 2.985, 512.96 ≤ x4 (μmm) ≤ 1187.04, 0.46 ≤ x5 (μmm) ≤ 251.91

Scenario 2

For this scenario, the search space of some design variables (x1, x2, x4, x5) was considered as integer. The intervals for the design variables are as follows: 1.203 ≤ x1 (L/min) ≤ 4.497, 505.56 ≤ x2 (μmm) ≤ 783.33, 2.215 ≤ x3 (mm) ≤ 2.985, 512.96 ≤ x4 (μmm) ≤ 1187.04, 0.46 ≤ x5 (μmm) ≤ 251.91{x1, x2, x4, x5} ∈ Integers

Scenario 3

In the third scenario, all design parameters were taken as only certain specific values determined in the experimental set. For this study, each design variable had 24 different levels. Due to implementing regression models for 24 different levels taking time regarding optimization, each design parameter's level is chosen as four specified values: minimum, maximum, middle, and the design parameters that performed the best results in the experimental study. The design parameters and their level values are; coolant flow rate (x1) ∈ {1.203, 2.850, 3.103, 4.497}, height of the first pin-fin (x2) ∈ {650.00, 772.22, 783.33, 1505.56}, distance from the vortex generator (x3) ∈ {2.215, 2.600, 2.659, 2.985}, width of the first pin-fin (x4) ∈ {512.96, 850.00, 1005.56, 1187.04}, distance of the vortex generator from surface (x5) ∈ {0.46, 113.89, 134.26, 251.91}.

Table 3. Design points regarding with input and output parameters [15]

Run Order	coolant flow rate (x1) (L/min)	height of the first pin-fin (x2) (μmm)	distance from the vortex generator (x3) (mm)	width of the first pin-fin (x4) (μmm)	distance of the vortex generator from surface (x5) (μmm)	IGBT temperature (°C)
1	2.723	650.00	2.748	642.6	81.67	82.68
2	1.203	527.78	2.748	979.63	47.22	106.65
3	2.977	683.33	2.778	953.70	80.93	80.42
4	1.457	672.22	2.896	746.30	40.06	98.18
5	4.370	605.56	2.215	1109.26	83.27	75.3
6	2.850	738.89	2.837	512.96	147.96	76.73
7	4.243	594.44	2.393	824.07	220.80	74.6
8	2.090	516.67	2.274	850.00	134.26	92.22
9	1.837	750.00	2.926	1187.04	119.44	85.66
10	2.343	761.11	2.511	668.52	76.98	80.65
11	1.710	583.33	2.867	1057.41	217.59	95.13
12	2.597	783.33	2.363	927.78	0.46	78.9
13	3.483	627.78	2.452	1083.33	161.30	78.28
14	2.217	572.22	2.481	798.15	251.91	88.34
15	3.863	550.00	2.719	875.93	35.00	77.77
16	3.230	727.78	2.600	564.81	99.81	76.03
17	1.583	638.89	2.689	1161.11	164.51	95.71
18	1.330	705.56	2.630	590.74	55.62	97.9
19	4.117	561.11	2.807	772.22	180.43	76.16
20	4.497	538.89	2.333	616.67	158.83	74.88
21	1.963	505.56	2.956	538.89	82.41	80.72
22	3.610	716.67	2.244	720.37	110.19	74.58
23	3.103	772.22	2.659	1005.56	113.89	74.36
24	3.737	694.44	2.985	1031.48	91.67	76

3. Results and Discussion

This study established a mathematical relationship between design parameters (coolant flow rate (x1), height of the first pin-fin (x2), distance from the vortex generator (x3), width of the first pin-fin (x4) and distance of the vortex generator from surface (x5)), and output parameter (IGBT temperature). The goal was to identify the values of these design parameters that minimize the IGBT temperature using the most effective model.

Table 4 presents the performance of various neuro-regression models in terms of their R^2 values (for training, testing, and validation phases) and their boundedness check (maximum and minimum values). The R^2 values during training are notably high across all models, with some achieving values close to 1.0. This suggests that the models exhibit a strong fit to the training data. However, such high values may indicate potential overfitting, where the model may not generalize well to unseen data.

In the testing and validation phase, several models yield negative R^2 values (e.g., LR: -0.541896, SOTNR: -8.17925), implying poor performance and possibly inverse predictions relative to the data trend. Particularly in the SOTNR model, this discrepancy may indicate substantial overfitting.

The maximum and minimum values across the models reveal that some models produce extreme bounds (e.g., the minimum value for SOTNR: 1.78333×10^{10}), indicating that these models may generate highly varied or extreme outputs. This wide prediction range points to a tendency toward volatility in some models.

The FOLN model demonstrates commendable performance across multiple evaluation criteria, particularly in terms of its R^2 values and boundedness. The model achieves high R^2 values in the training (0.99805), testing (0.996986), and validation phases (0.99921), indicating a consistently strong fit and predictive capability across different data subsets. Such uniformly high R^2 values suggest that the FOLN model not only learns the training data effectively but also generalizes well to unseen data, avoiding overfitting issues commonly observed in other models.

Regarding boundedness, the FOLN model maintains a prediction range with maximum and minimum values of 105.094 and 65.7673, respectively. This bounded range suggests a stable prediction behavior. The FOLN model's boundedness further supports its robustness, as it operates within a controlled range, contrasting with models that exhibit high variance in output values.

Among the models in Table 4,the FOLN model only demonstrates a balance between model fitness and prediction stability. For this reason, it is selected as an objective function in the optimization process to minimize IGBT temperature.

Table 4. Result of the Neuro-Regression Models in Terms of R^2 and Boundedness

Model	R^2Training	R^2Testing	R^2Validation	Max	Min
L	0.997574	0.880102	0.952265	105.559	60.8362
LR	0.999749	-0.541896	0.903765	∞	∞
SON	1.	0.384109	-1.01635	125.852	36.4097
SONR	0.999493	0.83447	0.45114	182.503	-3.5922*10^9
FOTN	0.999301	0.519079	0. .91273	110.303	58.3124
FOTNR	0.999854	-1.0012	0.83765	4.64839*10^6	3.82897*10^6
SOTN	0.999845	-0.268708	-0.0235936	108.566	44.027
SOTNR	0.999936	-8.17925	-16.0617	1.70706*10^15	1.78333*10^10
FOLN	*0.99805*	*0.996986*	*0.99921*	*105.094*	*65.7673*
FOLNR	0.999662	-1.85905	-2.08456	1.95554*10^7	2.77389*10^6
SOLN	1.	-1.39353	-1.38238	339.14	154.896
SOLNR	0.999875	-0.192595	-0.355909	4.01139*10^7	33.6077
H (FOLN+SON)	1.	-0.305234	0.314625	118.633	30.6786
H (FOLN*L)	0.999701	0.446418	0.937696	112.363	50.9868

Table 5 presents the results of optimization scenarios for the FOLN model, with a focus on achieving minimum Insulated-Gate Bipolar Transistor (IGBT) temperatures across various optimization algorithms: DE, SA, RS, and NM. The findings indicate the effectiveness and stability of the FOLN model in identifying optimal designs under diverse conditions.

In scenario 1, across all algorithms (MDE, MSA, MRS, MNM), the minimum IGBT temperature achieved is consistent at 65.7673°C, with the suggested design values for parameters x1 to x5 remaining identical. This outcome indicates a convergence across optimization methods toward a common design that minimizes temperature.

When the search space of some design variables (x1, x2, x4, x5) is considered an integer in scenario 2, slight variations appear between algorithms. For instance, MDE and MSA yield a minimum temperature of 68.4517°C, while MRS and MNM result in slightly higher temperatures of 68.7299°C and 71.365°C, respectively. The recommended parameter values exhibit minor differences by algorithms, suggesting some sensitivity in the model's design variable recommendations depending on the optimization technique.

In Scenario 3, under all design parameters are taken as only certain specific values determined in the experimental set, four algorithms consistently converge to the minimum IGBT temperature of 65.7673°C with same design parameters. This convergence among the algorithms suggests that the optimal result has been attained. A comparison with the experimental results from the reference study supports this inference. While the experimentally obtained minimum temperature was 74.36°C, the present study achieves a significantly lower minimum temperature of 65.7673°C through modeling and optimization.

In conclusion, this consistency reinforces the FOLN model's suitability for applications requiring precise thermal management within defined parameter boundaries.

Table 5. Results of optimization problems for FOLN model considering minimum IGBT temperature.

Objective Function	Scenario Number	Constrains	Optimization Algorithm	Minimum IGBT Temperature (°C)	Suggested Design
FOLN	1	1.203 ≤ x1 ≤ 4.497, 5 505.56≤ x2 ≤ 783.33 2.215 ≤ x3 ≤ 2.985 512.96 ≤ x4 ≤ 1187.04 0.46 ≤ x4 ≤ 251.91	DE	65.7673	x1 -> 4.497, x2 -> 783.33, x3 -> 2.985, x4 -> 512.96, x5 -> 0.46
			SA	65.7673	x1 -> 4.497, x2 -> 783.33, x3 -> 2.985, x4 -> 512.96, x5 -> 0.46
			RS	65.7673	x1 -> 4.497, x2 -> 783.33, x3 -> 2.985, x4 -> 512.96, x5 -> 0.46
			NM	65.7673	x1 -> 4.497, x2 -> 783.33, x3 -> 2.985, x4 -> 512.96, x5 -> 0.46
	2	1.203 ≤ x1 ≤ 4.497, 5 505.56≤ x2 ≤ 783.33 2.215 ≤ x3 ≤ 2.985 512.96 ≤ x4 ≤ 1187.04 0.46 ≤ x4 ≤ 251.91 {x1, x2, x4, x5} ∈ Integers	DE	68.4517	x1 -> 4, x2 -> 783, x3 -> 2.985, x4 -> 513, x5 -> 1
			SA	68.4517	x1 -> 4, x2 -> 783, x3 -> 2.985, x4 -> 513 x5 -> 1
			RS	68.7299	x1 -> 4, x2 -> 778, x3 -> 2.92473, x4 -> 513, x5 -> 1
			NM	71.365	x1 -> 4, x2 -> 707, x3 -> 2.985, x4 -> 826, x5 -> 211
	3	x1 = 1.203 || x1 = 2.850 || x1 = 3.103 || x1 = 4.497, x2 =505.56 || x2 = 650.00 || x2 = 772.22 || x2 = 783.33, x3 = 2.215 || x3 = 2.600 || x3 = 2.659 || x3 = 2.985, x4 = 512.96 || x4 = 850.00 || x4 = 1005.56 || x4 = 1187.04, x5 = 0.46 || x5 = 113.89 || x5 = 134.26 || x5 = 251.91	DE	65.7673	x1 -> 4.497, x2 -> 783.33, x3 -> 2.985, x4 -> 512.96, x5 -> 0.46
			SA	65.7673	x1 -> 4.497, x2 -> 783.33, x3 -> 2.985, x4 -> 512.96, x5 -> 0.46
			RS	65.7673	x1 -> 4.497, x2 -> 783.33, x3 -> 2.985, x4 -> 512.96, x5 -> 0.46
			NM	65.7673	x1 -> 4.497, x2 -> 783.33, x3 -> 2.985, x4 -> 512.96, x5 -> 0.46

4. Conclusion

This study highlights the critical role of thermal management in optimizing power electronics systems, specifically those employing IGBT components. By focusing on minimizing the IGBT temperature as the objective function, the optimization framework employed key design variables such as coolant flow rate (x1), height of the first pin-fin (x2), distance from the vortex generator (x3), width of the first pin-fin (x4) and distance of the vortex generator from surface (x5). Standard methods that use limited regression models often ignore nonlinear effects and are ineffective for optimizing thermal management for cooling systems of power electronics modules. This study introduces a new way to model the relation between cooling system design parameters and IGBT temperature by combining artificial neural networks (ANN) with regression techniques. This approach, called neuro-regression, selects the best models from linear, rational, logarithmic, polynomial, trigonometric, and hybrid types based on criteria R^2 and boundedness check. The FOLN neuro-regression model emerged as the most effective in achieving a balance between high predictive accuracy and model boundedness across training, testing and validation datasets.

The results indicate that when the FOLN model was selected as the objective function, the Differential Evolution, Simulated Annealing, Random Search, and Nelder-Mead algorithms found the minimum IGBT temperature to be 65.7673°C. This temperature is significantly lower than the minimum temperature of 74.36°C reported in experimental studies.

This outcome suggests that the FOLN model is particularly well-suited for applications necessitating precise and robust thermal control. Moreover, the consistency observed across different optimization algorithms emphasizes the result's robustness, as each algorithm converged to the same minimum temperature. This convergence validates the model's efficacy for thermal management in power electronics.

Future studies may further explore applying the FOLN model across a broader range of conditions to enhance predictive performance and thermal management strategies in advanced electronics systems.

Statements & Declarations

Competing Interests

"The authors declare that they have no known competing financial interests or personal relationships that could have appeared to influence the work reported in this paper. The authors have no relevant financial or non-financial interests to disclose."

Conflict of Interest

"The authors declare that they have no conflict of interest."

Author Contribution

Melih Savran, Conceptualization, Methodology, Software, Validation, Formal Analysis, Investigation, Data curation, Project Administration, Writing – Original Draft, Writing – Review & Editing, Visualization; Ece Nur Yüncü, Conceptualization, Software, Validation, Formal Analysis, Investigation, Data curation, Writing – Original Draft, Visualization; Levent Aydın, Conceptualization, Methodology, Software, Validation, Formal Analysis, Investigation, Data curation, Supervision, Project Administration, Writing – Review & Editing;

Availability of Data and Materials

The authors confrm that the data supporting the fundings of this study are available within the article.

Ethical Approval

All authors have previously approved this paper and judged that there is no ethical infringement.

Consent to Participate and Publish

All authors would like to declare that they have approved their participation and consent about the publication in this journal.

References

[1] F. Wang, J. Cao, Z. Ling, Z. Zhang, and X. Fang, "Experimental and simulative investigations on a phase change material nano-emulsion-based liquid cooling thermal management system for a lithium-ion battery pack," *Energy*, vol. 207, p. 118215, 2020.

[2] R. Sabbah, R. Kizilel, J. R. Selman, and S. Al-Hallaj, "Active (air-cooled) vs. passive (phase change material) thermal management of high power lithium-ion packs: Limitation of temperature rise and uniformity of temperature distribution," *Journal of Power Sources*, vol. 182, no. 2, pp. 630-638, 2008.

[3] Y. Song and B. Wang, "Survey on reliability of power electronic systems," *IEEE Transactions on Power Electronics*, vol. 28, no. 1, pp. 591-604, 2013.

[4] H. Zou, W. Wang, G. Zhang, F. Qin, C. Tian, and Y. Yan, "Experimental investigation on an integrated thermal management system with heat pipe heat exchanger for electric vehicle," *Energy Conversion and Management*, vol. 118, pp. 88-95, 2016.

[5] H. Lambate, S. Nakanekar, and S. Tonapi, "Thermal characterization of the IGBT modules used in hybrid electric vehicles," in *Fourteenth Intersociety Conference on Thermal and Thermomechanical Phenomena in Electronic Systems (ITherm)*, 2014, pp. 1086-1091.

[6] J. He, V. Mehrotra, and M. C. Shaw, "Thermal design and measurements of IGBT power modules: Transient and steady state," in *Conference Record of the 1999 IEEE Industry Applications Conference. Thirty-Fourth IAS Annual Meeting*, vol. 2, 1999, pp. 1440-1444.

[7] Z. Huang, T. An, F. Qin, Y. Gong, Y. Dai, and P. Chen, "Effect of the thermal contact resistance on the heat dissipation performance of the press-pack IGBT module," in *2022 23rd International Conference on Electronic Packaging Technology (ICEPT)*, 2022, pp. 1-4.

[8] A. S. Bahman, K. Ma, and F. Blaabjerg, "A lumped thermal model including thermal coupling and thermal boundary conditions for high-power IGBT modules," *IEEE Transactions on Power Electronics*, vol. 33, no. 3, pp. 2518-2530, 2018.

[9] F. Dong, Y. Feng, Z. Wang, and J. Ni, "Effects on thermal performance enhancement of pin-fin structures for insulated gate bipolar transistor (IGBT) cooling in high voltage heater system," *International Journal of Thermal Sciences*, vol. 146, p. 106106, 2019.

[10] R. V. Rao and V. K. Patel, "Thermodynamic optimization of cross flow plate-fin heat exchanger using a particle swarm optimization algorithm," *International Journal of Thermal Sciences*, vol. 49, no. 9, pp. 1712-1721, 2010.

[11] S. M. Lee and K. Y. Kim, "Multi-objective optimization of arc-shaped ribs in the channels of a printed circuit heat exchanger," *International Journal of Thermal Sciences*, vol. 94, pp. 1-8, 2015.

[12] M. Mishra, P. K. Das, and S. Sarangi, "Optimum design of crossflow plate-fin heat exchangers through genetic algorithm," *International Journal of Heat Exchangers*, vol. 5, no. 2, pp. 379-402, 2004.

[13] M. Mishra and P. K. Das, "Thermoeconomic design-optimisation of crossflow plate-fin heat exchanger using genetic algorithm," *International Journal of Exergy*, vol. 6, no. 6, pp. 237-252, 2009.

[14] W. T. Han, L. H. Tang, and G. N. Xie, "Performance comparison of particle swarm optimization and genetic algorithm in rolling fin-tube heat exchanger optimization design," in *Proceedings of the ASME Summer Heat Transfer Conference*, 2008, pp. 5-10.

[15] F. Pourfattah and M. Sabzpooshani, "On the thermal management of a power electronics system: Optimization of the cooling system using genetic algorithm and response surface method," *Energy*, vol. 232, p. 120951, 2021.

[16] İ. Polatoğlu, L. Aydın, B. Ç. Nevruz, and S. Özer, "A novel approach for the optimal design of a biosensor," *Analytical Letters*, vol. 53, no. 9, pp. 1428-1445, 2020.

[17] R. L. Haupt and S. E. Haupt, *Practical Genetic Algorithms*, 2nd ed., John Wiley & Sons, 2004.

[18] M. Bilal, M. Pant, H. Zaheer, L. Garcia-Hernandez, and A. Abraham, "Differential Evolution: A review of more than two decades of research," *Engineering Applications of Artificial Intelligence*, vol. 90, p. 103479, 2020.

[19] S. S. Fan, Y. C. Liang, and E. Zahara, "A genetic algorithm and a particle swarm optimizer hybridized with Nelder–Mead simplex search," *Computers & Industrial Engineering*, vol. 50, no. 4, pp. 401-425, 2006.

[20] M. Savran and L. Aydın, "Natural frequency and buckling optimization considering weight saving for hybrid graphite/epoxy-sitka spruce and graphite-flax/epoxy laminated composite plates using stochastic methods," *Mech Adv Mater Struct*, vol. 30, no. 13, pp. 2637-2650, 2023. https://doi.org/10.1080/15376494.2021.1875390.

[21] M. Savran, L. Aydın, A. Ayaz, and T. Uslu, "A new strategy for manufacturing, modeling, and optimization of 3D printed polylactide based on multiple nonlinear neuro regression analysis and stochastic optimization methods," *Proc Inst Mech Eng Part E J Process Mech Eng*, 2024. https://doi.org/10.1177/09544089241272909.

Appendix

Table 6. Full form of fitted models given in Table 4 for IGBT temperature minimization

L	$Y = 134.038 - 7.87285\,x1 - 0.0350987\,x2 - 3.84166\,x3 + 0.0052639\,x4 - 0.00609842\,x5$
LR	$Y = (-56968.1 + 9808.6\,x1 - 1.10747\,x2 + 13287.9\,x3 + 13.2699\,x4 - 61.2884\,x5) / (-701.641 + 127.019\,x1 - 0.0295636\,x2 + 160.471\,x3 + 0.169625\,x4 - 0.731965\,x5)$
SON	$Y = 143.16 - 26.1213\,x1 - 0.266133\,x1^2 + 0.205037\,x2 + 0.0164272\,x1\,x2 - 0.000215368\,x2^2 - 18.958\,x3 + 3.16074\,x1\,x3 + 0.0316068\,x2\,x3 - 6.10672\,x3^2 - 0.0526772\,x4 - 0.00426426\,x1\,x4 - 0.000106816\,x2\,x4 + 0.0345683\,x3\,x4 + 6.44028 * 10^{-6} x4^2 - 0.272179\,x5 + 0.0666481\,x1\,x5 - 0.000173512\,x2\,x5 - 0.118958\,x3\,x5 + 0.000406931\,x4\,x5 + 0.000532985\,x5^2$
SONR	$Y = (0.999998 + 1.00097\,x1 + 1.01073\,x1^2 + 1.18699\,x2 + 1.59093\,x1\,x2 + 8.07745\,x2^2 + 0.998744\,x3 + 0.999468\,x1\,x3 + 1.09109\,x2\,x3 + 0.992578\,x3^2 + 1.41276\,x4 + 2.01127\,x1\,x4 + 0.653814\,x2\,x4 + 1.19341\,x3\,x4 - 2.6552\,x4^2 + 0.973255\,x5 + 0.983887\,x1\,x5 +$

	$26.9875\,x2\,x5 + 0.545355\,x3\,x5 + 32.2588\,x4\,x5 + 8.93178\,x5^2) / (1.0129 + 1.03098\,x1 + 0.564842\,x1^2 - 10.509\,x2 + 16.1285\,x1\,x2 - 0.0135889\,x2^2 + 1.13578\,x3 + 1.33672\,x1\,x3 + 0.959568\,x2\,x3 + 1.6953\,x3^2 - 28.6864\,x4 - 7.66247\,x1\,x4 + 0.141888\,x2\,x4 - 3.19273\,x3\,x4 - 0.034077\,x4^2 + 7.05449\,x5 + 15.0197\,x1\,x5 + 0.586826\,x2\,x5 + 50.0506\,x3\,x5 + 0.032533\,x4\,x5 - 0.0767997\,x5^2)$
FOTN	$Y = -15.9216 + 7.46982\,Cos[x1] - 0.53304\,Cos[x2] - 87.6255\,Cos[x3] + 3.45563\,Cos[x4] - 5.72392\,Cos[x5] + 8.78887\,Sin[x1] - 2.18344\,Sin[x2] + 55.7862\,Sin[x3] + 0.443394\,Sin[x4] - 0.265043\,Sin[x5]$
FOTNR	$Y = (-0.730588 + 3.91013\,Cos[x1] + 1.92254\,Cos[x2] + 2.31712\,Cos[x3] + 0.309367\,Cos[x4] + 1.69828\,Cos[x5] + 4.18388\,Sin[x1] + 2.25224\,Sin[x2] + 0.0157777\,Sin[x3] + 4.34981\,Sin[x4] + 3.5477\,Sin[x5]) / (-0.0652036 + 0.0572789\,Cos[x1] + 0.0230747\,Cos[x2] - 0.0244729\,Cos[x3] - 0.000143375\,Cos[x4] + 0.0243629\,Cos[x5] + 0.0523375\,Sin[x1] + 0.0282922\,Sin[x2] + 0.0261709\,Sin[x3] + 0.0541034\,Sin[x4] + 0.0437403\,Sin[x5])$
SOTN	$Y = -47.3662 + 13.0646Cos[x1] - 63.5034Cos[x1]^2 + 2.56338Cos[x2] - 47.6764Cos[x2]^2 - 436.355Cos[x3] - 85.6018Cos[x3]^2 + 3.40693Cos[x4] - 57.3509Cos[x4]^2 - 3.14863Cos[x5] - 63.4364Cos[x5]^2 + 1.11839Sin[x1] - 60.9763Sin[x1]^2 - 0.102909Sin[x2] - 45.5672Sin[x2]^2 + 41.4972Sin[x3] + 139.775Sin[x3]^2 + 1.48926Sin[x4] - 45.5672Sin[x4]^2 + 1.84843Sin[x5] - 72.5961Sin[x5]^2$
SOTNR	$Y=(5.06164 + 0.909237Cos[x1] + 1.62149Cos[x1]^2 + 4.89529Cos[x2] + 0.713049Cos[x2]^2 - 3.13559Cos[x3] + 5.15071Cos[x3]^2 + 7.27358Cos[x4] + 0.649242Cos[x4]^2 + 8.37598Cos[x5] + 0.962236Cos[x5]^2 + 9.14495Sin[x1] + 4.44015Sin[x1]^2 - 1.426Sin[x2] + 9.76099Sin[x2]^2 + 1.76466Sin[x3] + 0.910924Sin[x3]^2 - 3.48212Sin[x4] + 9.76099Sin[x4]^2 + 4.65247Sin[x5] + 5.0994Sin[x5]^2)/(-0.470253 + 0.0554459Cos[x1] + 0.303031Cos[x1]^2 + 0.0464251Cos[x2] - 0.0150328Cos[x2]^2 - 0.831807Cos[x3] - 0.398776Cos[x3]^2 + 0.0428974Cos[x4] + 0.0192471Cos[x4]^2 + 0.145946Cos[x5] + 0.197603Cos[x5]^2 + 0.127331Sin[x1] + 0.226716Sin[x1]^2 - 0.00448057Sin[x2] + 0.0552804Sin[x2]^2 - 0.834104Sin[x3] + 0.928524Sin[x3]^2 - 0.0553128Sin[x4] + 0.0552804Sin[x4]^2 - 0.0048026Sin[x5] + 0.332144Sin[x5]^2)$
FOLN	$Y = 205.583 - 21.4628\,Log[x1] - 15.1221\,Log[x2] - 8.89083\,Log[x3] + 0.497759\,Log[x4] + 0.21157\,Log[x5]$
FOLNR	$Y = (-3235.77 + 668.333\,Log[x1] - 13.0274\,Log[x2] + 734.962\,Log[x3] + 472.026\,Log[x4] - 211.339\,Log[x5]) / (-38.355 + 8.63867\,Log[x1] - 0.687913\,Log[x2] + 8.60961\,Log[x3] + 6.16418\,Log[x4] - 2.65231\,Log[x5])$
SOLN	$Y = 515.076 - 89.4979Log[x1] - 12.2692Log[x1]^2 + 155.474Log[x2] + 40.8295Log[x1]Log[x2] + 10.3467Log[x2]^2 - 1127.92Log[x3] + 35.5538Log[x1]Log[x3] + 119.958Log[x2]Log[x3] - 58.5787Log[x3]^2 - 53.6643Log[x4] - 37.03Log[x1]Log[x4] - 40.0015Log[x2]Log[x4] + 98.8895Log[x3]Log[x4] + 1.13931Log[x4]^2 + 5.57893Log[x5] + 11.8181Log[x1]Log[x5] - 50.2312Log[x2]Log[x5] - 55.7305Log[x3]Log[x5] + 53.933Log[x4]Log[x5] - 1.0972Log[x5]^2$
SOLNR	$Y = (-0.335514 - 0.927137Log[x1] - 1.39658Log[x1]^2 - 8.13074Log[x2] - 11.7381Log[x1]Log[x2] - 61.8455Log[x2]^2 - 0.248695Log[x3] - 0.482518Log[x1]Log[x3] - 7.36435Log[x2]Log[x3] - 0.316384Log[x3]^2 + 12.6517Log[x4] + 11.259Log[x1]Log[x4] + 75.8271Log[x2]Log[x4] + 12.8017Log[x3]Log[x4] + 97.142Log[x4]^2 - 7.39312Log[x5] - 9.95039Log[x1]Log[x5] - 56.4527Log[x2]Log[x5] - 7.26286Log[x3]Log[x5] + 42.0738Log[x4]Log[x5] - 40.8657Log[x5]^2)/ (-0.000139906 + 2.58557Log[x1] - 1.09347Log[x1]^2 - 6.58669Log[x2] - 17.3051Log[x1]Log[x2] - 12.3961Log[x2]^2 + 0.64661Log[x3] - 25.9045Log[x1]Log[x3] - 18.4784Log[x2]Log[x3] + 14.4391Log[x3]^2 - 8.55544Log[x4] + 23.5569Log[x1]Log[x4] + 17.504Log[x2]Log[x4] - 6.39485Log[x3]Log[x4] + 0.668614Log[x4]^2 - 2.53994Log[x5] - 3.78552Log[x1]Log[x5] + 20.5227Log[x2]Log[x5] + 36.3018Log[x3]Log[x5] - 23.9271Log[x4]Log[x5] - 0.375019Log[x5]^2)$
H (FOLN+SON)	$Y = 90.1139 + 0.442761x1 - 2.29539x1^2 + 0.0746876x2 + 0.0156922x1x2 - 0.000131892x2^2 - 3.71033x3 + 6.16279x1x3 + 0.0250583x2x3 - 4.80624x3^2 + 0.0418714x4 - 0.0109804x1x4 - 0.0000555408x2x4 + 0.0225954x3x4 - 0.0000395405x4^2 - 0.11773x5 + 0.0438845x1x5 - 0.000164884x2x5 - 0.139816x3x5 + 0.000415728x4x5 + 0.000370671x5^2 - 39.8574Log[x1] + 8.66859Log[x2] - 26.899Log[x3] - 5.74012Log[x4] - 0.201207Log[x5]$
H (FOLN*L)	$Y = (37.0467 + 2.02402\,x1 - 0.0444288\,x2 - 6.24084\,x3 - 0.0585529\,x4 - 0.000602118\,x5)\,(-19.2654 + 0.230805\,Log[x1] + 1.18382\,Log[x2] + 0.215925\,Log[x3] + 1.41784\,Log[x4] + 0.000906653\,Log[x5])$